

# Edge preserving phase unwrapping using graph cuts

Gonalo Valado & Jos M. Bioucas-Dias

*Instituto de Telecomunicaes, Instituto Superior Tcnico, Torre Norte, Piso 10, Av. Rovisco Pais, 1049-001 Lisboa, Portugal, Email:{gvaladao, bioucas}@lx.it.pt*

**Keywords:** phase unwrapping, interferometric synthetic aperture radar (InSAR), integer optimization, graph cuts, image processing

**ABSTRACT:** This paper addresses the problem of recovering the absolute phase from modulo- $2\pi$  phase, the so-called phase unwrapping (PU) problem. PU is a key step in several imaging technologies, namely, interferometric synthetic aperture radar (InSAR), and interferometric synthetic aperture sonar (InSAS). There, the topographic information is encoded in the phase of a complex valued image with a (different) multiple  $2\pi$  ambiguity on each pixel. Some kind of PU procedure must then be employed to find the actual absolute phase and, from there, the desired topographic data. We establish a phase unwrapping algorithm, in the vein of the minimization of the  $L^p$  norm of phase differences, that is similar to our previous one published in [1]; the main contribution of this paper is to bring in adaptive edge preservation to the original surface recovering. A set of experimental results illustrates the effectiveness of the algorithm.

## 1 INTRODUCTION

Phase is an important property of many classes of signals, namely in interferometric synthetic aperture radar (InSAR) and interferometric synthetic aperture sonar (InSAS), where two or more antennas are used to measure the phase between them and the terrain; the topography is then obtained, from elementary geometry, as a function of the difference between those phases [2].

In spite of phase being a crucial information, either in InSAR as in InSAS, the acquisition system can only measure phase modulo- $2\pi$ , the so-called principal phase value, or wrapped phase. Formally, we have

$$\phi = \psi + 2k\pi, \tag{1}$$

where  $\phi$  is the true phase value (the so-called absolute value),  $\psi$  is the measured (wrapped) modulo- $2\pi$  phase value, and  $k \in \mathbb{Z}$  an integer number of wavelengths [3].

Phase unwrapping (PU) is the process of recovering the absolute phase  $\phi$  from the wrapped phase  $\psi$ . This is, however, an ill-posed problem, if no further information is added. In fact, an assumption taken by most phase unwrapping algorithms is that the absolute value of phase differences between neighbouring pixels is less than  $\pi$ , the so-called Itoh condition [4]. If this assumption is not violated, the absolute phase can be easily determined, up to a constant. Itoh condition might be violated if the true phase surface is discontinuous, or if only a noisy version of the wrapped phase is available. In either cases, PU becomes a very difficult problem, to which much attention has been devoted [3], [5].

Phase unwrapping approaches belong to one of these following classes: path following [6], minimum  $L^p$  norm [7], Bayesian [8], and parametric modeling [9].

Path following algorithms apply line integration schemes over the wrapped phase image, and basically rely on the assumption that Itoh condition holds along the integration path. A representative technique employed to handle these inconsistencies is the so-called *residues branch cuts* [6].

Minimum  $L^p$  norm methods exploit the fact that the differences between absolute phases of neighbour pixels, are equal to the wrapped differences between correspondent wrapped phases, if Itoh condition is met. Thus, these methods try to find a phase solution  $\phi$  for which  $L^p$  norm of the difference between absolute phase differences and wrapped phase differences (so a second order difference) is minimized. This is, therefore, a global minimization in the sense that all the observed phases are used to compute a solution. With  $p=2$  we have a least squares method [10]. A drawback of the  $L^2$  norm is that this criterion tends to smooth discontinuities, unless they are provided as binary weights.  $L^1$  norm performs better than  $L^2$  norm in what discontinuity preserving is concerned. Such a criterion has been solved by Flynn [11], using network programming. With  $0 \leq p < 1$  the ability of preserving discontinuities is further increased at stake, however, of highly complex algorithms.

The Bayesian approach relies on a data-observation mechanism model, as well as a prior knowledge of the phase to be modelled. For instance in [12], a non-linear optimal filtering is applied, while in [13] an InSAR observation model is considered, and is taken into account not only the image phase, but also the *backscattering coefficient* and *correlation factor* images, which are jointly recovered from InSAR image pairs.

Finally, parametric algorithms constrain the unwrapped phase to a parametric surface. Low order polynomial surfaces are used in [9]. Very often in real applications just one polynomial is not enough to describe accurately the complete surface. In such cases the image is partitioned and different parametric models are applied to each partition [9].

### 1.1 Proposed approach

This paper establishes a phase unwrapping algorithm in the vein of the minimum  $L^p$  norm class of PU algorithms. The corresponding optimization problem is herein considered in a similar way as in our previous work [1]. Accordingly we still call PUMF to the proposed PU algorithm. The main contribution of the present approach is to introduce (Sect. 4.2) adaptive edge preservation of the original absolute phase discontinuities, i.e., unwrap the surface without explicitly supplying information on discontinuities locations. This is done using a class of non-convex clique potentials used, since long, in image processing [14]. It should be noted that however we adopt a practical point of view, not having a complete theoretical support for such an approach.

PUMF minimizes the  $L^p$  norm of the complete set of phase differences between neighbour pixels, with the constraint of being  $2\pi$ -congruent with wrapped phases. The integer optimization problem we are led to is solved by a series of binary elementary optimizations as presented in [5] for the  $\mathbb{Z}\pi\mathbf{M}$  algorithm. The present approach casts, however, the optimization problem as a max-flow/min-cut calculation on a certain graph, building on energy minimization results presented in [15]. The developed algorithm is valid (strictly) for  $p \geq 1$ , for which the  $L^p$  norm is a convex function.

## 2 PROBLEM FORMULATION

Adopting the representation used in [5], Fig. 1 shows a pixel and its four neighbours along with the variables  $h$  and  $v$  signalling horizontal and vertical discontinuities respectively.

The  $L^p$  norm of the difference between neighbouring pixels phases,  $2\pi$ -congruent with wrapped phases, is given by

$$E(\mathbf{k}|\psi) = \sum_{i,j \in \mathbb{Z}_1} |\Delta\phi_{ij}^h|^p \bar{v}_{ij} + |\Delta\phi_{ij}^v|^p \bar{h}_{ij}, \quad (2)$$

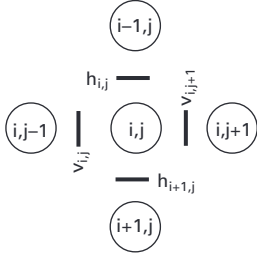


Figure 1. Representation of the pixel  $(i, j)$  and its first order neighbours along with the variables  $h$  and  $v$  signalling horizontal and vertical discontinuities respectively.

where  $(\cdot)^h$  and  $(\cdot)^v$  denotes pixel horizontal and vertical differences given by

$$\Delta\phi_{ij}^h = [2\pi(k_{ij} - k_{ij-1}) - \Delta\psi_{ij}^h], k \in \mathbb{Z} \quad (3)$$

$$\Delta\phi_{ij}^v = [2\pi(k_{ij} - k_{i-1,j}) - \Delta\psi_{ij}^v], k \in \mathbb{Z} \quad (4)$$

$$\Delta\psi_{ij}^h = \psi_{ij-1} - \psi_{ij} \quad (5)$$

$$\Delta\psi_{ij}^v = \psi_{i-1,j} - \psi_{ij}, \quad (6)$$

with  $p \geq 0$ ,  $\psi$  being the wrapped (observed) phase,  $\bar{h}_{ij} = 1 - h_{ij}$  and  $\bar{v}_{ij} = 1 - v_{ij}$  ( $h_{ij}, v_{ij} \in \{0, 1\}$ ) being binary horizontal and vertical discontinuities respectively, and  $(i, j) \in \mathbb{Z}_1$  where  $\mathbb{Z}_1 = \{(i, j) : i = 1, \dots, M, j = 1, \dots, N\}$ , and with  $M$  and  $N$  denoting the number of lines and columns respectively (i.e., the usual image pixel indexing 2D grid).

Our purpose is to find the integer image  $\mathbf{k}$  that minimizes energy (2),  $\mathbf{k}$  being such that  $\phi = 2\pi\mathbf{k} + \psi$ , where  $\phi$  is the estimated unwrapped image;  $\mathbf{k}$  is the so-called *wrap-count* image. To achieve this goal, we compute a series of graph flow calculations for which efficient max-flow/min-cut algorithms exist.

### 3 MINIMIZING $E$ BY A SEQUENCE OF BINARY OPTIMIZATIONS

The following lemma, taken from [5], assures that if the minimum of  $E(\mathbf{k}|\psi)$  is not yet reached, then there exists a binary image  $\delta\mathbf{k}$  (i.e., the elements of  $\delta\mathbf{k}$  are all 0 or 1) such that  $E(\mathbf{k} + \delta\mathbf{k}|\psi) < E(\mathbf{k}|\psi)$ .

**Lemma 1** *Let  $\mathbf{k}_1$  and  $\mathbf{k}_2$  be two wrap-count images such that*

$$E(\mathbf{k}_2|\psi) < E(\mathbf{k}_1|\psi). \quad (7)$$

*Then, if  $p \geq 1$ , there exists a binary image  $\delta\mathbf{k}$  such that*

$$E(\mathbf{k}_1 + \delta\mathbf{k}|\psi) < E(\mathbf{k}_1|\psi). \quad (8)$$

*Proof.* The proof follows the same line of the one given in the appendix of [5] for  $p = 2$ , using the convexity of  $|x|^p$  with respect to  $x$ , for  $p \geq 1$ .

According to Lemma 1, we can iteratively compute  $\mathbf{k}^{t+1} = \mathbf{k}^t + \delta\mathbf{k}$ , where  $\delta\mathbf{k} \in \{0, 1\}^{MN}$  minimizes  $E(\mathbf{k}^t + \delta\mathbf{k}|\psi)$ , until the minimum energy is reached.

### 3.1 Mapping Binary Optimizations onto Graph Min-Cuts

Let  $k_{ij}^{t+1} = k_{ij}^t + \delta k_{ij}^t$  be the wrap-count at time  $t + 1$  and pixel  $(i, j)$ . Introducing  $k_{ij}^{t+1}$  into (3) and (4), making some simple manipulations and introducing the obtained expressions into (2), we can rewrite energy  $E(\mathbf{k}|\psi)$  as a function of binary variables  $\delta k_{ij}^t$ , i.e.,

$$E(\mathbf{k}|\psi) = \sum_{ij \in \mathbb{Z}_1} \underbrace{|2\pi(\delta k_{ij}^t - \delta k_{ij-1}^t) + a^h|^p \bar{v}_{ij}}_{E_h^{ij}(x_{ij-1}, x_{ij})} + \underbrace{|2\pi(\delta k_{ij}^t - \delta k_{i-1j}^t) + a^v|^p \bar{h}_{ij}}_{E_v^{ij}(x_{i-1j}, x_{ij})}, \quad (9)$$

where  $x_{ij} = \delta k_{ij}^t$ ,  $a^h = 2\pi(k_{ij}^t - k_{ij-1}^t) - \Delta\psi_{ij}^t$ , and  $a^v = 2\pi(k_{ij}^t - k_{i-1j}^t) - \Delta\psi_{ij}^t$ .

For simplicity, let us denote for a moment terms  $E_h^{ij}$  and  $E_v^{ij}$  by  $E^{ij}(x_k, x_l)$ . We have thus,  $E^{ij}(0, 0) = |a|^p \bar{d}_{ij}$ ,  $E^{ij}(1, 1) = |a|^p \bar{d}_{ij}$ ,  $E^{ij}(0, 1) = |2\pi + a|^p \bar{d}_{ij}$ , and  $E^{ij}(1, 0) = |-2\pi + a|^p \bar{d}_{ij}$ , where  $a$  represents  $a_h$  or  $a_v$  and  $\bar{d}_{ij}$  represents  $\bar{h}_{ij}$  or  $\bar{v}_{ij}$ .

So, we also have  $E^{ij}(0, 0) + E^{ij}(1, 1) = 2|a|^p \bar{d}_{ij}$ , and  $E^{ij}(0, 1) + E^{ij}(1, 0) = (|-2\pi + a|^p + |2\pi + a|^p) \bar{d}_{ij}$ . For  $p \geq 1$ , terms  $E(x_k, x_l)$  verify  $E^{ij}(0, 0) + E^{ij}(1, 1) \leq E^{ij}(0, 1) + E^{ij}(1, 0)$ , this following from the convexity of  $E(\mathbf{k}|\psi)$ .

We are now in conditions of stating that energy (2) is *graph-representable*, using Theorem 4.1 stated in [15]. The proof of that theorem (also given in the cited work) shows how to construct the representative graph. First, build vertices and edges corresponding to each pair of neighbouring pixels, and then join these graphs together based on the additivity theorem also given in [15].

So, for each energy term  $E_h^{ij}$  and  $E_v^{ij}$  [see expression (9)], we construct an “elementary” graph with four vertices  $\{s, t, v, v'\}$ , where  $\{s, t\}$  represents source and the sink, common to all terms, and  $\{v, v'\}$  represents the two pixels involved ( $v$  being the left (up) pixel and  $v'$  the right (down) pixel). Following very closely [15], we define a directed edge  $(v, v')$  with the weight  $E(0, 1) + E(1, 0) - E(0, 0) - E(1, 1)$ . Moreover, if  $E(1, 0) - E(0, 0) > 0$  we define an edge  $(s, v)$  with the weight  $E(1, 0) - E(0, 0) - E(0, 0)$  or, otherwise, we define an edge  $(v, t)$  with the weight  $E(0, 0) - E(1, 0)$ . In a similar way for vertex  $v'$ , if  $E(1, 1) - E(1, 0) > 0$  we define an edge  $(s, v')$  with weight  $E(1, 1) - E(1, 0) > 0$  or, otherwise, we define an edge  $(v', t)$  with the weight  $E(1, 0) - E(1, 1)$ .

Also in [15] it is shown that there is a one-to-one mapping between the configuration of  $(x_1, \dots, x_n)$ , and cuts leaving the source and the sink in disconnected components; furthermore, the cost of the cut is the value of the energy on that configuration. Therefore, minimizing the energy corresponds to computing the max-flow. As we have shown above, building on results from [5] and from [15], we can iteratively find an energy minimum through binary optimizations, based on max-flow calculation on a certain graph.

Algorithm 1 shows the pseudo-code for the Phase Unwrapping Max-Flow (PUMF) algorithm<sup>1</sup>.

## 4 EXPERIMENTAL RESULTS

The results presented in this section were obtained by a MATLAB coding of the PUMF algorithm [max-flow is coded in C++ (see [16])].

In Sect. 4.1 we present two difficult representative PU problems that PUMF is able to efficaciously attack. In Sect. 4.2 we present the results for a PU problem that we solve with a minor variation on PUMF, further enhancing discontinuity preserving capabilities. It should be stressed that only on the second PU problem of Sect. 4.1 we provide information on discontinuities<sup>2</sup>.

<sup>1</sup> The authors acknowledge Vladimir Kolmogorov for the max-flow/min-cut C++ code made available on the web.

<sup>2</sup> Even so, just a minor region of the total discontinuity information available.

---

Algorithm 1 (PUMF) Graph cuts based phase unwrapping algorithm.

---

**Initialization:**  $k \equiv k' \equiv 0$ , possible\_improvement  $\equiv 1$

```

1: while possible_improvement do
2:   Compute  $E(0, 0)$ ,  $E(1, 1)$ ,  $E(0, 1)$ , and  $E(1, 0)$  {for every horizontal and vertical pixel pairs}.
3:   Construct elementary graphs and merge them to obtain the main graph.
4:   Compute the min-cut  $(S, T)$  { $S$ - source set;  $T$ -sink set}.
5:   for all pixel  $(i, j)$  do
6:     if pixel  $(i, j) \in S$  then
7:        $k'_{i,j} = k_{i,j} + 1$ 
8:     else
9:        $k'_{i,j} = k_{i,j}$  {remains unchanged}
10:    end if
11:  end for
12:  if  $E(k'| \psi) < E(k| \psi)$  then
13:     $k = k'$ 
14:  else
15:    possible_improvement = 0
16:  end if
17: end while

```

---

#### 4.1 PUMF results

Figure 2(a) displays a noisy phase image to be unwrapped; it was synthesized from a Gaussian elevation height of  $14\pi$  rad, and standard deviations  $\sigma_i = 15$  and  $\sigma_j = 10$  pixels. This synthesis consists of generating a pair of SAR complex images, given the desired absolute phase surface and pair coherence [17]; this is done according to the InSAR observation model adopted in [5]. The wrapped phase image is then obtained, by computing the product of one image by the complex conjugate of the other, and finally taking the argument. The correlation coefficient,  $0 \leq \alpha \leq 1$ , of the associated InSAR pair is, in this case,  $\alpha = 0.95$ . This value is low enough to induce a large number of phase jumps, making the unwrapping a very difficult task. Figure 2(b) shows the corresponding unwrapped surface by PUMF with  $p = 2$ . We can see that in a few iterations (ten) PUMF successfully accomplishes the unwrapping. The corresponding energy decreasing is shown in Fig. 2(c).

Figure 2(d) shows a wrapped phase image analogous to 2(a), but now the original phase corresponds to a (simulated) InSAR acquisition for a (real) high-relief mountainous area inducing, therefore, many discontinuities and posing a very difficult PU problem. Figure 2(e) shows the unwrapped surface by PUMF. It should be stressed that this is a tough phase unwrapping problem, and thus a (minor) quality map was supplied as an input discontinuity map to the algorithm. This quality map labels each difference as 0 or 1 according, respectively, to whether there is, or there is not, a discontinuity. PUMF accomplished the unwrapping, taking 20 iterations, with  $p = 1$ . With this setting, the accuracy of the unwrapping is given by an error norm of 87 (squared rads). The error norm obtained with the WLS (Weighted Least Squares [18]) algorithm is 1270. This difference is due to the fact that the WLS algorithm relaxes the discrete problem to the continuum, before minimizing and then going back to the discrete domain, whereas the PUMF solves exactly the integer minimization problem. The error norm obtained with the QG (Quality Guided [19]) algorithm, a specially indicated one for this kind of PU problem, was 85 which confirms the state-of-the-art competitive accuracy of PUMF in this PU problem<sup>3</sup>.

#### 4.2 A variation into discontinuity preservation

Several families of discontinuity preserving potentials have been successfully used in image processing [14], [20]. Here we also very briefly tested such approach on PUMF using, instead of  $|\cdot|^p$ , a

---

<sup>3</sup> The error norms were calculated over the subset (of the entire image) defined by the quality map, plus a one pixel erosion in order to cut-off mask border pixels that usually have problems.



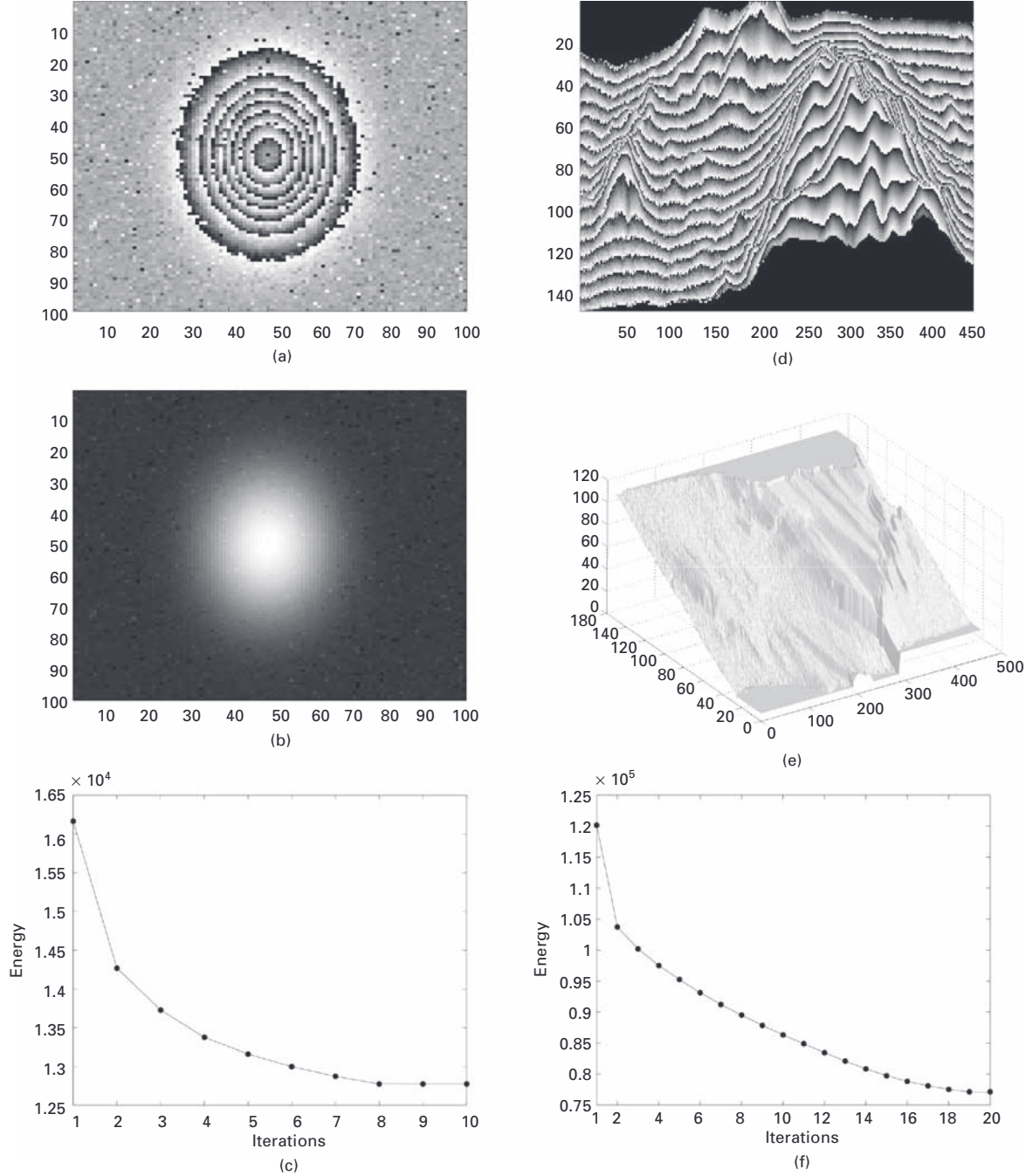


Figure 2. (a) Wrapped phase image (rad) from a Gaussian absolute phase surface of height  $14\pi$  rad and standard deviations  $\sigma_i = 15$  and  $\sigma_j = 10$ . The correlation coefficient of the associated pair is 0.95. (b) Image in (a) unwrapped by PUMF ( $p = 2$ , 10 iterations). (c) Energy decreasing for the unwrapping of image in (a). (d) Wrapped phase image (rad) from a simulated InSAR acquisition for an area around Long's Peak, Colorado (data distributed with book [3]). (e) Image in (d) unwrapped by PUMF ( $p = 1$ , 20 iterations). (f) Energy decreasing for the unwrapping of image in (d).

potential given by  $V(\cdot) = -\frac{1}{1+|\cdot|^2}$ , taken from [21]. Figure 3(a) depicts the graph of  $V(\cdot)$ . As it is non-convex, we have not theoretical support to use PUMF with such a potential. Nevertheless good results have been obtained. Figure 3(b) displays a phase image to be unwrapped; it was synthesized from an original absolute phase surface formed by two equal size planes with slopes 0 and 1 rad/

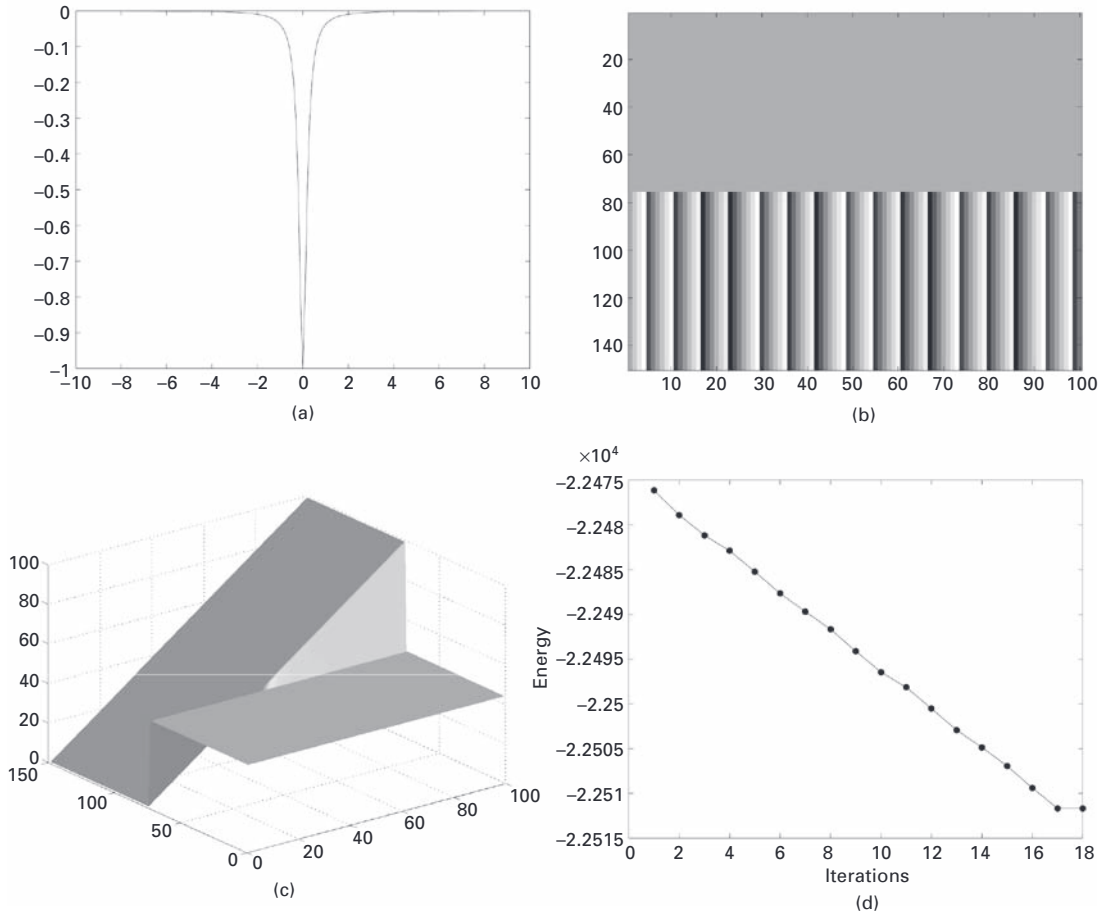


Figure 3. (a) Discontinuity preserving potential. (b) Wrapped sheared planes. (c) The resulting unwrapped phase surface (perfectly identical to the original). (d) Energy decreasing for the unwrapping process.

pixel (maximum height is 99 rad). The wrapped image is (again) generated according to an InSAR observation statistic (see, e.g., [5]) with correlation coefficient 1.0. The original absolute phase surface has a sharp discontinuity (between the two sheared planes) that needs to be preserved in the unwrapping process. Figure 3(c) shows the corresponding unwrapped surface by PUMF with  $p = 2$ , taking 18 iterations and, approximately, 4 seconds in a 2GHz PC. We can see that PUMF successfully accomplishes a perfect unwrapping. In Fig. 3(d) it can be seen the energy minimization along the PU process.

## 5 CONCLUDING REMARKS

We introduced a new PU algorithm that computes exactly the  $2\pi$  congruent minimum  $L^p$  norm of any linear function of the phase neighbouring differences, for convex norms. This class of energy functions includes the usual norms used in PU.

The proposed algorithm is iterative, solving, in each iteration, a minimization over a binary *move* (each pixel allowed to remain unchanged or to be incremented by  $2\pi$ ). This minimization is implemented efficiently by exploiting recent results from [15] on energy minimization via max-flow/min-cut computations on certain graphs. In the experiments shown, the proposed PUMF algorithm competes with state-of-the-art methods.

An open issue is the performance of PUMF for edge preserving potentials which are however

non-convex. Using such a potential, instead of the  $L^p$  norm we were able to successfully blindly unwrap a surface having a sharp discontinuity to be preserved. This is, however, an issue for future research.

## REFERENCES

1. Bioucas-Dias, J. and Valadão, G. Phase unwrapping via graph cuts. In *Proceedings of the Second Iberian Conference - IbPRIA2005*, volume 1, pages 360–367, Estoril, Portugal, June 2005.
2. Rosen, P., Hensley, S., Joughin, I., Li, F., Madsen, S., Rodriguez, E. and Goldstein, R. Synthetic aperture radar interferometry. *Proceedings of the IEEE*, 88(3): 333–382, March 2000.
3. Ghiglia, D. and Pritt, M. *Two-Dimensional Phase Unwrapping. Theory, Algorithms, and Software*. John Wiley & Sons, New York, 1998.
4. Itoh, K. Analysis of the phase unwrapping problem. *Applied Optics*, 21(14), 1982.
5. Dias, J. and Leitão, J. The  $\mathbb{Z}\pi M$  algorithm for interferometric image reconstruction in SAR/SAS. *IEEE Transactions on Image Processing*, 11: 408–422, April 2002.
6. Goldstein, R., Zebker, H. and Werner, C. Satellite radar interferometry: Two-dimensional phase unwrapping. In *Symposium on the Ionospheric Effects on Communication and Related Systems*, volume 23, pages 713–720. Radio Science, 1988.
7. Ghiglia, D. and Romero, L. Minimum  $L^p$  norm two-dimensional phase unwrapping. *Journal of the Optical Society of America*, 13(10): 1999–2013, 1996.
8. Nico, G., Palubinskas, G. and Datcu, M. Bayesian approach to phase unwrapping: theoretical study. *IEEE Transactions on Signal Processing*, 48(9): 2545–2556, Sept. 2000.
9. Friedlander, B. and Francos, J. Model based phase unwrapping of 2-D signals. *IEEE Transactions on Signal Processing*, 44(12): 2999–3007, 1996.
10. Fried, D. Least-squares fitting a wave-front distortion estimate to an array of phase-difference measurements. *Journal of the Optical Society of America*, 67(3): 370–375, 1977.
11. Flynn, T. Two-dimensional phase unwrapping with minimum weighted discontinuity. *Journal of the Optical Society of America A*, 14(10): 2692–2701, 1997.
12. Leitão, J. and Figueiredo, M. Absolute phase image reconstruction: A stochastic non-linear filtering approach. *IEEE Transactions on Image Processing*, 7(6): 868–882, June 1997.
13. Dias, J. and Leitão, J. Simultaneous phase unwrapping and speckle smoothing in SAR images: A stochastic nonlinear filtering approach. In *EUSAR'98 European Conference on Synthetic Aperture Radar*, pages 373–377, Friedrichshafen, May 1998.
14. Blake, A. and Zisserman, A. *Visual Reconstruction*. MIT Press, Cambridge, M.A., 1987.
15. Kolmogorov, V. and Zabih, R. What energy functions can be minimized via graph cuts? *IEEE Transactions on Pattern Analysis and Machine Intelligence*, 26(2): 147–159, February 2004.
16. Boykov, Y. and Kolmogorov, V. An experimental comparison of min-cut/max-flow algorithms for energy minimization in vision. *IEEE Transactions on Pattern Analysis and Machine Intelligence*, 26(9): 1124–1137, 2004.
17. Jakowatz, C., Wahl, D., Eichel, P., Ghiglia, D. and Thompson, P. *Spotlight-Mode Synthetic Aperture Radar: A Signal Processing Approach*. Kluwer Academic Publishers, Boston, 1996.
18. Ghiglia, D. and Romero, L. Robust two-dimensional weighted and unweighted phase unwrapping that uses fast transforms and iterative methods. *Journal of the Optical Society of America A*, 11: 107–117, 1994.
19. Lim, H., Xu, W. and Huang, X. Two new practical methods for phase unwrapping. In *Proceedings of the 1995 International Geoscience and Remote Sensing Symposium-IGARSS'95*, pages 196–198, Firenze, Italy, 1995.
20. Geman, S. and Geman, D. Stochastic relaxation, Gibbs distribution, and Bayesian restoration of images. *IEEE Trans. Pattern Anal. Machine Intell.*, 6: 721–741, 1984.
21. Geman, S. and McClure, D. Statistical methods for tomographic image reconstruction. In *Proceedings of the 46<sup>th</sup> Session of the International Statistical Institute*, pages 353–356. Bulletin of the ISI, Vol. 52, 1987.